Generating Proper Integrated Dynamic Models for Vehicle Mobility Using a Bond Graph Formulation

Loucas S. Louca, Jeffrey L. Stein and D. Geoff Rideout

The University of Michigan
Department of Mechanical Engineering, Automated Modeling Laboratory
G029 W.E. Lay Automotive Lab
Ann Arbor, MI 48109-2121

Email: cyl@umich.edu, stein@umich.edu and drideout@umich.edu

Keywords: Integrated Simulation, Model Reduction, Automated Modeling, Proper Models, Energy Metrics, and Vehicle Dynamics.

ABSTRACT

This work presents the development, validation, use and reduction of an integrated vehicle model composed of the engine, drivetrain and vehicle dynamics. Integrated models that include all vehicle subsystems are essential for many driving scenarios that induce rich dynamic responses. The model is developed with the assumption that it will be used for a wide range of excitations, and therefore, all possible complexity is included in the model, e.g., drivetrain flexibility and large rigid body motions. The bond graph formulation is used for model development because it facilitates the integration of component/subsystem models, provides the user with physical insight, and allows easy manipulation of models. The engine model is a steady state torque map generated from an engine thermodynamic model. The drivetrain consists of the torque converter, transmission and driveline. A nonlinear planar model of the vehicle is used to predict the dynamics in the longitudinal, heave and pitch degrees of freedom. For illustration, the model is configured for a Class VI, International 4700 series delivery truck, and implemented in the 20SIM modeling and simulation environment. The integrated vehicle simulation is validated against transient data measured on the proving ground.

An energy-based model reduction methodology is applied in order to produce proper vehicle models that provide more design insight and can be more computationally efficient. This provides a systematic approach to address the modeling assumptions and generate reduced models that are valid under specific scenarios. A reduced system model is generated, which produces results very similar to the full (baseline) model. In addition to its predictive quality, the utility of the reduced model to study trade-offs involved in redesigning components and control strategies for improved performance of the vehicle system is demonstrated.

1. INTRODUCTION

Vehicle design is a costly process that is initiated with a comprehensive analysis of the vehicle system in order to determine the desired characteristics of subsystems. This process is followed by detailed design of subsystems and components, and finally building and testing of prototypes. Development time and cost can be significantly reduced using simulation-based design. A predictive vehicle system simulation can allow the creation and testing of the virtual vehicle for a variety of conditions, and guide component design prior to building prototypes. The availability of a comprehensive vehicle simulation with high fidelity subsystem models also enables concurrent design, where changes in one component are reflected on the design of related components and subsystems. In addition, a predictive simulation can assist in quantifying parameters associated with subjective driver feel and overall driveability that are difficult to measure and yet very important for customer acceptance.

Previous attempts to model the entire vehicle system have been characterized by a variety of approaches, differing in the fidelity of individual models as well as the methodologies used to integrate the various subsystems. Early attempts were based on collections of look-up tables for the engine and drivetrain subsystems, and point mass vehicle dynamics models (Haley et al., 1979; Buck, 1981; Philips and Assanis, 1989)). These simulations can be very valuable for quick assessments of vehicle mobility, although they lack the ability to capture fast vehicle transients. Their other limitation is the fact that, for every new component, new look-up tables need to be generated through hardware testing, making them impractical to study non-existing designs. Caterpillar was among the first to attempt to marry a thermodynamic diesel engine cycle simulation with DYNASTY (Fluga, 1993).

Significant improvements in the integration methodology have since emerged based on object-oriented graphical programming environments, such as EASY5, MATLAB/SIMULINK and 20SIM. These computer environments allow more flexibility in connecting/interchanging models of components and subsystems, and they are appropriate for control type studies. A fully flexible, comprehensive and predictive transient vehicle system simulation needs to take advantage of both improved models and advanced simulation environments. Another requirement for having a predictive/accurate simulation is component modeling using physically based formulations like bond graphs. This characteristic allows the easy integration of models within a design optimization framework and more importantly, it helps engineers to gain physical insight into the system, which is critical for new system designs. Finally, the model accuracy must be assured by systematic algorithms that can reduce excessively complicated and computationally expensive system models. This is also true for the individual component and subsystem models.

In an attempt to use the techniques and simulation environments mentioned above, Assanis et al. (1999) developed a first generation high fidelity vehicle simulation that was configured for a 6x6 heavy-duty truck. A hierarchy of varying resolution models was built into a flexible, dynamic simulation system that could be tailored for specific simulation studies. The application of the complete vehicle simulation demonstrated the ability to predict the effect of engine system design changes on vehicle performance, as well as the complex interaction between the powertrain and the vehicle during highly transient maneuvers, e.g., hill climbing on wet road surface causing wheel slip.

The objectives of this work are to present the current developments of the integrated vehicle simulation for enhanced fidelity and flexibility, to validate its ability to predict engine and vehicle behavior during transients, and to illustrate the generation of varying complexity component models. Fidelity enhancements focus on realistic engine fuel controller, as well as physical models of the individual drivetrain and vehicle dynamics subsystems. The validation of the model is performed by comparing simulation predictions for an International class VI truck against data measured on the proving ground. Finally, systematic model reduction techniques are implemented in order to generate simpler models that are able to accurately and efficiently predict the system behavior.

The paper is organized as follows: first, a description the vehicle structure and subsystem models are provided in Section 2. Next, the integrated model validation is given in Section 3. Then, in Section 4, the energy-based metric is applied to the model in order to generate a reduced model, with which a parametric study is conducted. Finally, a discussion and set of conclusions are given in Sections 0 and 6, respectively.

2. VEHICLE MODEL STRUCTURE

The vehicle system is comprised of the engine, drivetrain and vehicle dynamics. The schematic of the vehicle system is given in Figure 1. The engine is connected to the torque converter (TC), whose output shaft is then coupled to the transmission (T), propeller shaft (PS), differential (D)

and two driveshafts (DS), coupling the differential with the driven wheels. The vehicle is rear driven and has solid front and rear axles with leaf spring suspension. This structure represents a diesel powered 4x2 delivery truck with a 4-speed automatic transmission, however, the same structure can be used for modeling most two axle vehicles after minimal modifications.

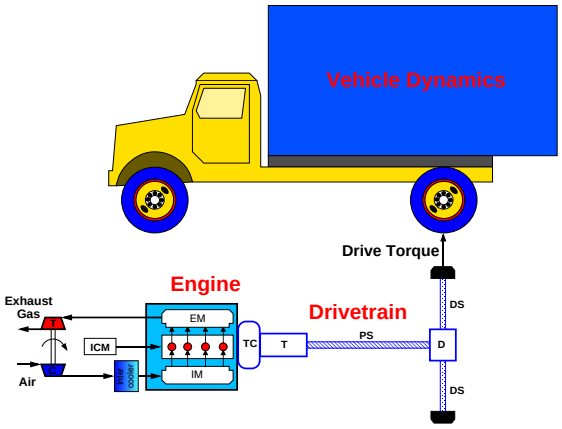

Figure 1: Schematic of the integrated vehicle system

The model is developed in the 20SIM modeling environment that supports hierarchical modeling and also allows the physical modeling of subsystems and components using the bond graph formulation. The model is developed with the intention of using the model reduction approach described in the background section. Therefore, all components and subsystems are "blindly" allowed to have the maximum possible complexity, i.e., all physical phenomena are included in the model without considering their significance to the system behavior. The system model complexity will be later addressed by applying the energy-based metric.

At the top level of the model hierarchy, we have the engine, drivetrain and vehicle dynamics excited by the environment. One source of excitation is the driver who controls the vehicle velocity through the gas and brake pedal (there is no clutch since we have an automatic transmission). The driver can also control the vehicle heading through the steering wheel, however, the steering input is neglected and the vehicle is constrained to move only on the pitch plane. The other excitation comes from the road, which is usually uneven and prescribes a velocity to the tires. The road excitation is applied to both front and rear tires as a function of their position. The top-level representation is shown in Figure 2. Notice that this top-level resembles the actual vehicle structure.

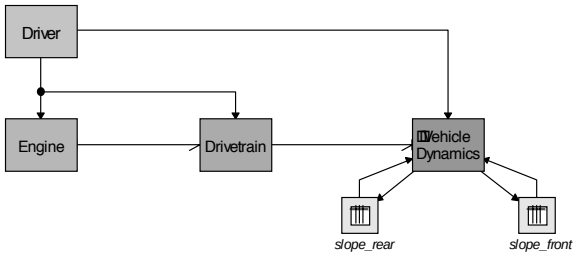

Figure 2: Top-level vehicle representation

2.1 Engine

The engine model includes the inertial effects of all rotating parts and energy losses due to friction, which are lumped into single port I and R elements, respectively. The engine brake torque is produced from a steady state lookup table as a function of the engine speed and fueling rate (see Figure 3). Typically, this table is obtained from measurements of the actual engine. However, because we wish to have the capability of studying the behavior of a vehicle with a new engine, a high fidelity model of a virtual engine is used to generate the lookup table. The engine model is comprised of multiple cylinder modules linked with external component modules for compressors and turbines, heat exchangers, air filters, and exhaust system elements. The engine cylinder model tracks the cylinder thermodynamic processes throughout a cycle as a function of crank angle. The specifications for the engine used in this work correspond to the International 7.3 L V8 engine type T444E.

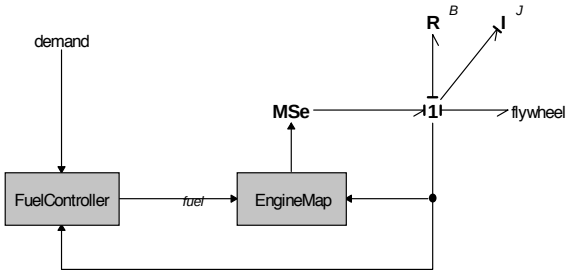

Figure 3: Engine subsystem

The engine power is controlled by the fuel injection controller. The diesel engine fuel injection controller provides the signal for the mass of fuel injected per cycle based on driver demand, environmental conditions and current engine operating conditions. Special functions include corrections for insufficient boost pressure, cold start, high altitude, and the governing function. More details of the engine subsystem are provided in the work by Assanis et al., 1999.

2.2 Drivetrain

The drivetrain consists of the torque converter, transmission, propshafts, differential, drive shafts, and shift logic. It provides the connection between the engine and the vehicle dynamics subsystems (see Figure 4). The torque converter input shaft, on one end, and the drive shaft, on the other end, are the connecting points for the engine and the vehicle dynamics models, respectively. The inputs are the engine speed and wheel rotational speed and the outputs the torque to the wheels and load torque on the engine. An additional input is the driver demand signal, which is used by the shift logic to determine if an upshift or downshift event is required. The specific elements used in the components are described below.

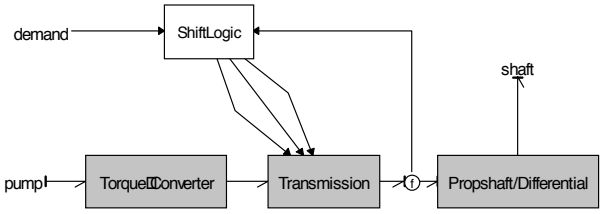

Figure 4: Drivetrain subsystem

2.2.1 Torque converter

The torque converter is the fluid clutch by which the engine is coupled to the transmission. The typical three-element converter consists of a pump, stator, and turbine. The pump is connected rigidly to the engine output shaft, and the turbine to the transmission input shaft. The stator is connected to the torque converter housing via a one-way clutch. The presence and arrangement of the stator cause the torque converter to act as a torque multiplication device when operating at low speed ratios, and as an approximately direct drive fluid coupling at higher speed ratios. The fluid coupling has characteristics of a gyrator (RMGY) since the pump and turbine torques are determined by the turbine and pump speeds. The model also includes the turbine inertia (see Figure 5).

The gyrator is a nonlinear and non-power conserving element that accounts for the energy losses due to the fluid circulation. The gyrator modulus is calculated from quasi-static experimental data. Two measured quantities define the nonlinear modulus: a) torque ratio (T_{ratio}) and b) capacity factor (K). These quantities are measured experimentally as a function of the speed ratio. The constitutive equations of the gyrator are:

$$\omega_{ratio} = \frac{\omega_{turbine}}{\omega_{pump}}, T_{pump} = \left(\frac{K(\omega_{ratio})}{\omega_{pump}}\right)^2, T_{turbine} = T_{ratio}(\omega_{ratio}) \cdot T_{pump} \quad (1)$$

The measured data of the capacity factor and torque ratio are curve fitted as a function of speed ratio in a piecewise manner and included in the constitutive law of the gyrator. This quasi-static torque converter model assumes that the torque converter is not subject to fast engine speed transients that occur during throttle steps. The torque converter model is thus a limiting factor at present.

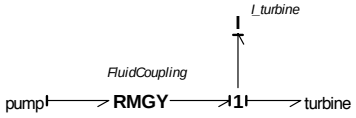

Figure 5: Torque converter component

2.2.2 Transmission

The central element of the transmission is a non-power conserving transformer that models gear efficiency and allows it to vary among different gears. The speed reduction in each gear is assumed ideal, while the torque multiplication is reduced by the appropriate gear efficiency factor. The transmission model consists of a series spring-inertia-spring arrangement and the non-power conserving transformer (gear ratio) in between (see Figure 6). In parallel with each spring is a viscous damper that gives a damping ratio of 5%. These ideal elements represent the equivalent inertia and compliance of the gears and shafts.

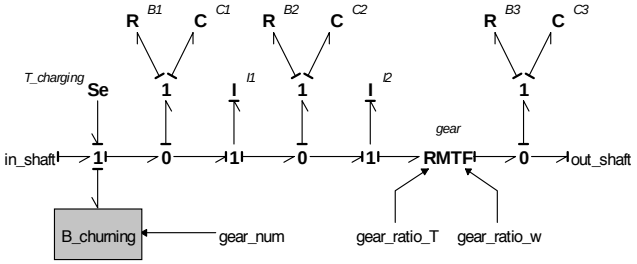

Figure 6: Transmission component

The transmission fluid churning losses are modeled as a variable nonlinear resistance (including linear and quadratic terms) which depends on the gear number. The charging pump is modeled as a constant torque loss represented by an effort source that independent of gear number or transmission speed.

2.2.3 Propshafts and differential

There are two propshafts, joined by a universal joint, which are modeled as an inertia-spring-inertia-spring-inertia series arrangement, again with small viscous damping. Following the propshafts is the differential, which includes an input compliance, axle inertia, and output compliance (see Figure 7). The model includes the cooler fluid churning losses for the differential/axle, which are modeled as an R element (including constant and linear terms). The differential is modeled as a non-power conserving transformer with ideal speed reduction but non-ideal torque multiplication based on a given gear efficiency.

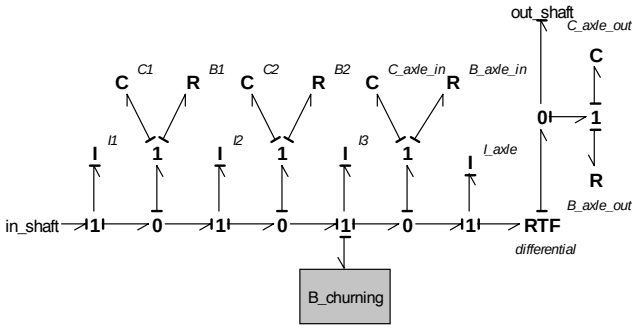

Figure 7: Propshafts and differential model

2.2.4 Shift logic

The inputs to the shift logic module are the transmission output shaft speed and the driver demand. The shift logic outputs the gear number, speed ratio and torque ratio. A chart such as the one shown in Figure 8, determines the current gear number, and whether or not an upshift or downshift event is to be initiated. The solid and dashed lines indicate upshift and downshift thresholds, respectively.

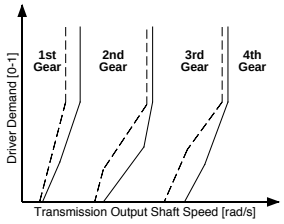

Figure 8: Gearshift logic map

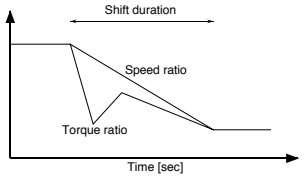

Figure 9: Blending functions

During a gearshift, the speed reduction and torque multiplication ratios vary from the initial to the final value according to blending functions. The blending functions model the torque and speed ratio variations that occur during the shift event, as clutches and bands engage and disengage. Typical shapes of blending functions are shown in Figure 9. The shift logic is described by a set of logical statements.

2.3 Vehicle Dynamics

The vehicle dynamics subsystem includes the wheels/tires, axles/suspensions and frame of the vehicle. The vehicle is modeled as a collection of rigid bodies that are allowed to move in the 2-dimensional space subject to forces/moments and rigid constraints (see Figure 10).

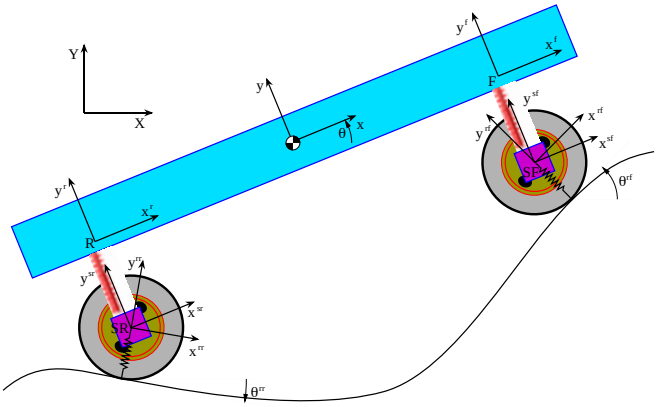

Figure 10: Half car model schematic

The forces/moments are physical elements, which act at specific points of two bodies, e.g., the rear suspension acts between point SR of the axle and point R of the frame. In addition, two bodies can be restrained to move only in a specific direction or trajectory by a rigid constraint, e.g., the front axle is constrained to move on the y^f-axis of the frame. The vehicle dynamics is connected to the drivetrain at the rear driven wheels. Previous research has developed models of a half car using the bond graph approach. For example, Pacejka and Tol (1983) developed a simplified linear model by assuming small pitch angles. In this work, we are interested in a wider range of pitch motion, which makes the suggested bond graph representation more complex and difficult to manipulate. Therefore, a hierarchical modeling approach is used. The vehicle is decomposed into the frame, front axle and front wheel, and rear axle and rear wheel as shown in Figure 11.

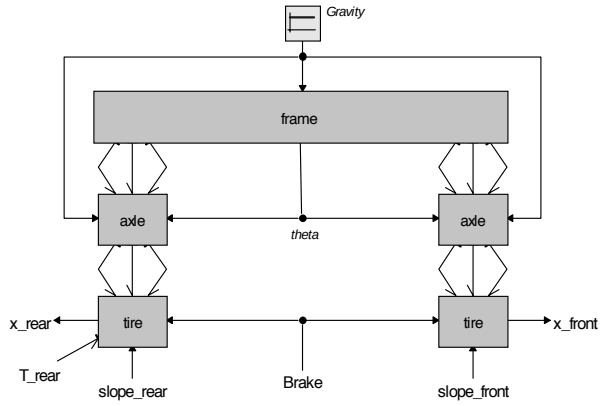

Figure 11: Vehicle dynamics subsystem

2.3.1 Frame

The frame is modeled as a rigid body that is allowed to move horizontally, vertically and to pitch. The bond graph of this component is depicted in Figure 12. Three inertial elements are used to represent the dynamics in the three degrees of freedom. The kinematics are described in a body fixed frame and represented by the modulated GY, which is the standard Eulerian junction structure for the 2-dimensional case. Gravity force is applied at the center of gravity (CG) location after transforming the CG velocity in the inertial (X, Y) frame. This transformation is a coordinate rotation around the out of plane axis and is given by Eq. (2). The frame also includes two points for connecting the front and rear axles. Each point is located at a constant position (x_F, y_F) and (x_R, y_R) relative to the CG. For example, the absolute velocity of the rear point, expressed in body fixed coordinates, is given by Eq. (3). Finally, the aerodynamic drag is modeled by a quadratic R element.

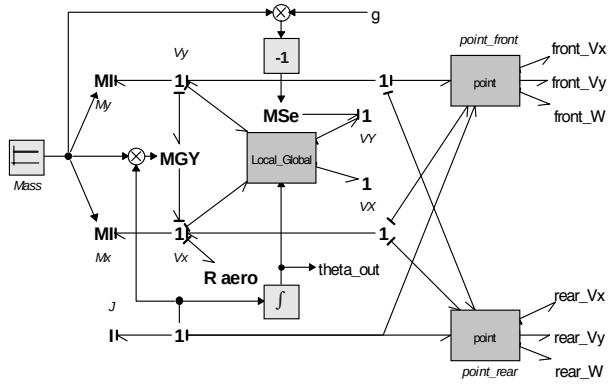

Figure 12: Frame component

$$\begin{Bmatrix} V_X \\ V_Y \end{Bmatrix} = \begin{bmatrix} \cos(\vartheta) & -\sin(\vartheta) \\ \sin(\vartheta) & \cos(\vartheta) \end{bmatrix} \bullet \begin{Bmatrix} V_x \\ V_y \end{Bmatrix} \quad (2)$$

$$V_x^R = V_x - \omega \cdot y_R$$
$$V_y^R = V_y + \omega \cdot x_R \quad (3)$$

2.3.2 Axle - Suspension

Each axle is modeled as a rigid body with its kinematics described in a body fixed frame. The axle is constrained by a rigid constraint to move on an axis that has its origin at the attachment point (F or R) and is perpendicular to the horizontal axis of the frame (x^f, y^f) or (x^r, y^r), respectively. In the bond graph shown in Figure 13, this constraint is realized by the modulated transformer (MTF), which describes a velocity constraint as in Eq. (3). The axle is also constrained by the suspension that is modeled as a linear spring and damper connected in parallel. Finally, the gravity force is applied to the axle through the transformation of the local velocities into the global frame. Note the inertial element *Mx* has derivative causality due to the rigid constraint defined by the MTF.

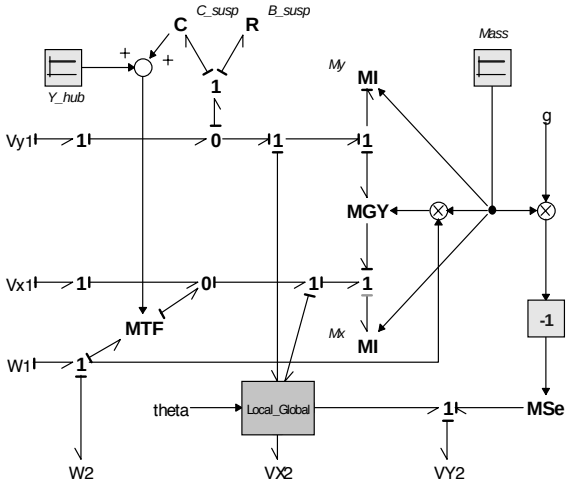

Figure 13: Axle-Suspension component

2.3.3 Wheel - Tire

This component includes the wheel dynamics and the interaction of the tire with the road. The wheel mass is lumped to the axle to avoid more kinematic constraints and derivative causality. The model includes the wheel moment of inertia and bearing viscous losses at the wheel hub (see Figure 14). The drive torque from the drivetrain is applied to the hub to accelerate the wheel. A simple brake model with viscous and coulomb friction is included to generate the required torque for decelerating and stopping the vehicle. In addition, the tire rolling resistance is added to the model as an additional source of energy losses.

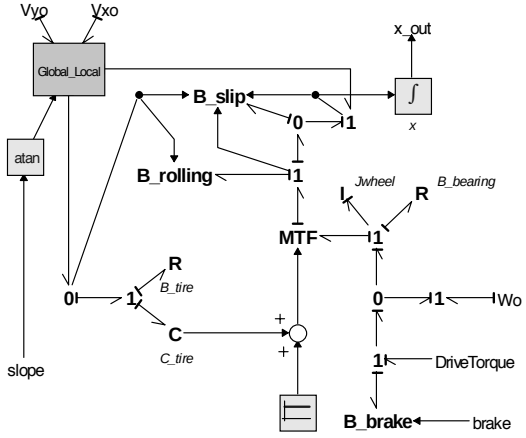

Figure 14: Wheel-Tire component

The tire in the vertical direction is modeled as a linear spring and damper connected in parallel. The model can also predict wheel lift off. The longitudinal traction force is calculated using the Pacejka model taken from the work of Pacejka and Bakker (1993). First, the axle velocity at point (SF or SR) is converted in a frame that is aligned with the road at the contact point. This coordinate transformation (similar as in Eq. (2)) gives the velocities of the contact point (SF or SR in the (x^{rf}, y^{rf}) or (x^{rr}, y^{rr}), respectively). Then, this velocity is used to calculate the wheel slip. Finally, the traction force is calculated as a nonlinear function of wheel slip and normal load. This function is given by the Pacejka model and its constants are estimated from measured data of the actual tire. In the bond graph notation, this behavior is modeled with a force-generating element that exhibits dissipative characteristics.

3. MODEL VALIDATION

This baseline model is first validated through comparisons of the simulated predictions with measurements obtained from the real vehicle on the proving grounds. The experimental data is limited to engine and vehicle speed histories. However, since these variables represent the result of complex engine and vehicle interactions, it is felt that the agreement between these two quantities would effectively validate the behavior of the entire system during such maneuvers.

The model is tested under one of the most dramatic transients – vehicle launch and acceleration at full load. The vehicle is initially at stand still, with brakes applied and the engine idling at 700 rpm. At t = 3 seconds, the brakes are released and driver demand is linearly ramped up to the maximum value in one second. The vehicle and engine response is tracked until the vehicle reaches 60 MPH. The comparison of predicted and measured engine and vehicle speed results is shown in Figure 15. The vehicle speed results show excellent agreement. The engine speed response indicates reasonable agreement across the overall profile, with the first two gear shifts actually occurring at the same time as predicted, and only the last one occurring slightly earlier on the simulated profile. Further, the predicted drop in engine speed during gearshifts closely matches the experimental results.

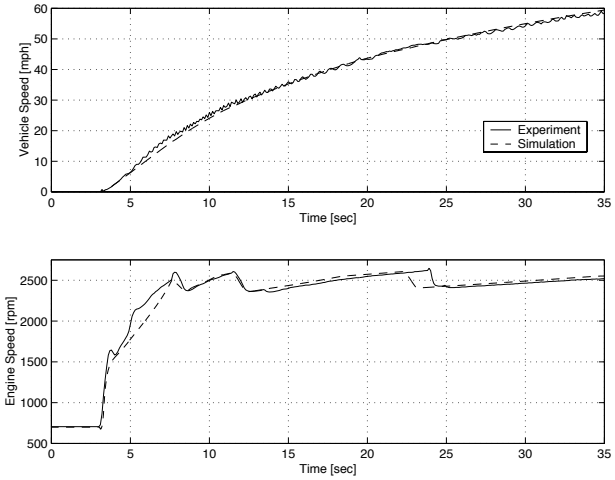

Figure 15: Simulated Vs measured data during the 0-60 MPH acceleration

4. MODEL REDUCTION

The model validation and design study results are generated from a model that has the maximum possible complexity (baseline model). To improve the simulation efficiency by eliminating elements that do not contribute to outputs of interest, while retaining design variables with physical meaning; an energy-based Model Order Reduction Algorithm (MORA) is applied to the baseline model. The application of MORA requires a model and set of parameters, which we already have, and a rich input to excite all the dynamics of the system for a given scenario.

The original work on the energy-based metric for model reduction (Louca et al., 1997) is briefly described here for convenience. The main idea behind this model reduction technique is to evaluate the "element activity" of the individual energy elements of a full system model under a stereotypic set of input and initial conditions. Element activity has units of energy, representing the amount of energy that flows in and out of the element over the given time. The energy that flows in and out of an element is a measure of how active this element is (how much energy passes through it), and consequently this quantity is termed activity. The activity of each energy element establishes a hierarchy for all the elements. Those elements below a user-defined threshold of acceptable level of activity are eliminated from the model, a reduced model is generated and a new set of governing differential equations is derived. More extensions and applications of the activity metric are given by Louca and Stein, 1998; Louca et al., 1998; Louca, 1998.

The selected scenario for the calculation of the activity is a full throttle acceleration from stand still on a flat road and then braking to bring the vehicle back to full stop. At the beginning, the engine is idling with the brakes applied, and then at t = 5 seconds the brakes are released and full throttle is applied. Finally, after 35 seconds of acceleration, the throttle is released and brakes are applied to stop the vehicle.

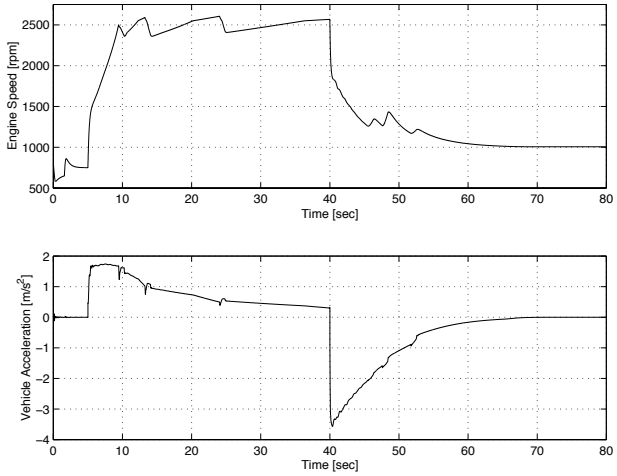

Figure 16: Vehicle response for the acceleration/braking maneuver

The baseline model is used to calculate the system response as it is performing this acceleration/braking maneuver. The response of the vehicle during this maneuver is shown in Figure 16 with some of the typical variables of interest. The simulation also generates the required outputs needed for the calculation of the power, the activity, and finally the activity index that MORA requires. There are 55 energy elements in the model. The time window used to calculate the activity is the time needed for the vehicle to complete both the acceleration and braking maneuver.

The sorted element activity indices and cumulative activity indices for this maneuver are plotted in Figure 17 and the numerical values given in the Appendix. Notice that the cumulative activity reaches approximately 80 percent after including the first five (5) most important elements. The most important element is the vehicle mass in the forward direction with 42% of the total activity. The least important elements are the viscous damping of the flexible shafts in the drivetrain.

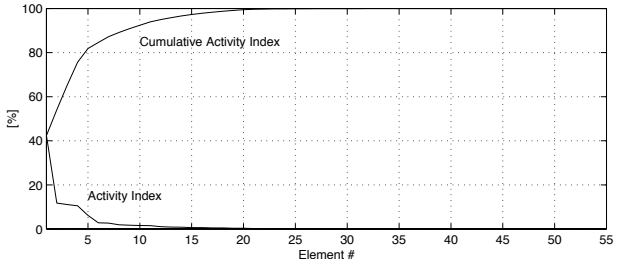

Figure 17: Sorted Activity Indices and Cumulative Index

A reduced model is generated based on the above activity index results. The element elimination starts with the least important element (Engine\B) and continues with elements of higher activity. The last 38 elements eliminated from the model, resulting in reduced model that maintains 98.34% of the total activity. Most of the eliminated elements are the inertial, compliant and resistive effects of the shafts in the drivetrain. Other eliminated elements include the suspension and tire compliances, frame moment of inertia and inertia of the axles in the vertical direction. Finally, the charging and churning losses of the transmission are not important and therefore eliminated from the model. The elimination of these low activity elements produces a reduced model that has no pitch or vertical motion, which might be expected since we have a heavy vehicle

accelerating on a flat road. The reduced model only includes the frame and axle masses in the longitudinal direction along with the aerodynamic drag. In addition, the wheel inertias, rolling resistances, brake losses and tire slips are included. Finally, the churning losses of the differential, the losses of the transmission and differential gear efficiency and engine inertia have high activity, and therefore, are included in the reduced model.

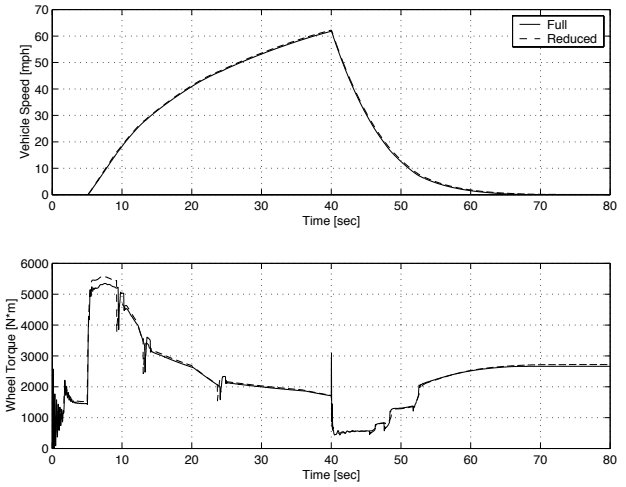

Figure 18: Comparsion of the full and reduced model

A reduced model is first generated by eliminating the energy elements suggested by the activity metric (only the 17 most active elements are included in the reduced model). Then, this reduced model is used to predict the vehicle behavior over the same acceleration/braking maneuver. Figure 18 compares the vehicle speed and wheel torque as predicted by the reduced model versus the full baseline model. The predictions from the two models are almost identical for the vehicle speed. There is only a small discrepancy in the prediction of the drive torque. Notice that the responses are quite similar, except form the high frequency effects that are eliminated from the reduced model. The computational efficiency of the reduced model is improved by a factor of 2.5 when using the Vode-Adams variable-step integration algorithm.

4.1 Design study

The potential usefulness of the reduced integrated vehicle model as a design tool is explored through a parametric study. The study assesses the possible side effects associated with modification of control strategies in an attempt to improve overall vehicle performance. More specifically the effect of varying the duration of the gearshift event is studied. The duration of the shift event is varied in order to study possible effects on system response and driver comfort. The original duration (0.8 seconds) is varied by +/- 0.4 seconds and the "full-throttle" acceleration simulation is repeated. Changing the shift duration essentially scales the blending function in Figure 9 along the horizontal axis. A shorter shift duration represents quicker engagement and disengagement of the transmission clutches and bands, during the speed and torque phases of the shift.

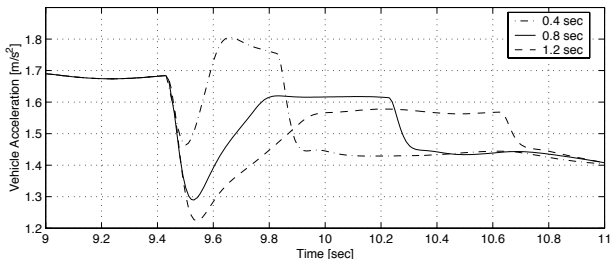

Figure 19: Variations of vehicle acceleration with shift duration

The variation in the maximum vehicle acceleration during the shift from first gear to second is shown in Figure 19. The maximum value of forward acceleration increases as the shift duration decreases. In addition, the acceleration loss during the first phase of the shift event is reduced, due to the faster engagement of the clutches.

5. DISCUSSION

Modeling of an integrated dynamic system using a hierarchical approach is advantageous. A systematic approach minimizes modeling mistakes by breaking the system model into small subsystems and components that are manageable in size and complexity. The same components can be used repeatedly without having to build models of the same part twice. For example, the axle component in the vehicle dynamics subsystem is built once and used for both the front and rear axle. In addition, with hierarchical modeling, models of the same component with different complexity can be easily interchanged without having to change the remaining structure of the model. Finally, the bond graph language is ideal for this type of modeling since component model compatibility is made clear with the notion of ports and causality.

Model validation of the baseline model demonstrates good agreement with the experimental data. However, the first five seconds should be examined more closely, since that interval is significantly influenced by turbocharger lag and system dynamics. The sharp increase and the first spike on the measured engine speed profile are associated with the extreme dynamics in the torque converter. The engine overspeeds somewhat before the torque converter is able to provide feedback in the form of the increased pump torque, felt by the engine as the reaction torque. The whole event associated with that initial spike takes place during one crankshaft revolution, and it would take some finite time to accelerate the fluid inside the torque converter. The quasi-steady TC model is not capable of capturing such a dynamic process and hence responds instantaneously, keeping the engine speed down at the beginning of the simulation.

The outcome of the model reduction procedure may seem trivial to an expert in vehicles, however it provides critical information to a modeler with not much experience in vehicle modeling. In addition, identifying the elements that contribute the most to a specific maneuver is in general not a trivial task. Generating the proper model with MORA provides critical information to the engineer. Perhaps the most readily assessable benefit is that the activity identifies the important parameters (elements) relative to a particular scenario. Thus, even if the model is not reformulated into reduced form, having a rank ordered list of the parameter importance directs the designer towards the design features that can produce the greatest effect on the system. Another benefit of ranking parameter importance is that the time and effort (cost) of obtaining model parameters can be reduced. A full model can be created with low precision parameter values. Then, upon learning which parameters are important, resources can be directed into obtaining higher precision values of the important parameters. Design optimization would also benefit from the knowledge of parameter importance by eliminating the need to perturb otherwise unimportant model parameters.

A reduced model that retains physically meaningful parameters facilitates design studies. In the shift duration example, shorter shift duration (0.4 seconds) resulted in crisper acceleration. While greater acceleration may be desirable from a performance standpoint, the increased rate of change of forward acceleration during the shorter shift event may adversely affect ride quality and driver comfort. Increasing driver comfort through prolonged shift durations raises questions about clutch wear and long term durability, as the clutch slip occurs over a longer period. The ability to evaluate such trade-offs between factors affecting performance, driver comfort and feel, and durability can be a valuable aid in designing a new, specialized application, e.g., commuter bus, off road vehicle, etc.

6. SUMMARY AND CONCLUSIONS

Development, validation and use of an integrated system simulation in concert with a model reduction algorithm are presented in this paper. In the vehicle system described herein, a quasi-static engine model is integrated with drivetrain and vehicle dynamics models of proper

complexity for the simulation objectives. The simulation is configured to predict the dynamic behavior of an International 4700 4x2 truck, powered by a turbocharged, intercooled engine, and equipped with a four speed automatic transmission. The complete vehicle simulation structure is implemented in 20SIM. Vehicle launch from standstill and subsequent full load acceleration to 60 MPH shows very good agreement between model predictions and experimental measurements. The vehicle speed profile is predicted with great accuracy. The overall engine speed history shows very good agreement, with the exception of the very beginning of the transient. Discrepancies are attributed to the fidelity of the torque converter model.

The model complexity is addressed with an energy-based metric. Results show that by removing 37 out of the 55 elements of the full model, a reduced model is produced which generates almost identical predictions as the baseline model. For acceleration and braking of this vehicle, the pitch motion does not need to be included in the model. Moreover, the computational efficiency of the reduced model is significantly improved. Finally, a design study indicates the potential of the simulation to be a useful engineering tool for the efficient and systematic evaluation of vehicle design trade-offs.

7. ACKNOWLEDGMENT

The authors gratefully acknowledge the support of this work by the U.S. Army Tank Automotive Command (ARC DAAE 07-94-Q-BAA3) through the Automotive Research Center (ARC), University of Michigan. Polat Sendur, University of Michigan, is recognized for his initial work on modeling the torque converter and transmission. The contributions of Dan Grohnke, Steve Gravante and Xinqun Gui of International Truck and Engine Corporation are also gratefully acknowledged.

8. REFERENCES

20SIM, 2000. 20SIM Pro Users' Manual, Version 3.1. The University of Twente - Controllab Products B.V. Enschede, The Netherlands.

Assanis, D., Bryzik, W., Chalhoub, N., Filipi, Z., Henein, N., Jung, D., Liu, X., Louca, L., Moskwa, J., Munns, S., Overholt, J., Papalambros, P., Riley, S., Rubin, Z., Sendur, P., Stein, J., Zhang, G., 1999. Integration and Use of Diesel Engine, Driveline and Vehicle Dynamics Models for Heavy Duty Truck Simulation, SAE paper 1999-01-0970.

Buck, R.E., 1981. A Computer Program (HEVSIM) for Heavy Duty Vehicle Fuel Economy and Performance Simulation—Volume 2: Users' Manual, U. S. DOT Document # DOT-HS-805-911.

Haley, P. W., M.P. Jurkat, and P.M. Brady, 1979. NATO Reference Mobility Model - NRMM, Edition I, User's Guide, Volume I, Operational Modules, Technical report 12503, US Army Tank-Automotive Research and Development Command, Warren, Michigan.

Fluga, E.C., 1993. Modeling of the Complete Vehicle Powertrain Using ENTERPRISE, SAE Paper 931179.

Karnopp, D.C., D.L. Margolis, and R.C. Rosenberg, 1990. System Dynamics: A Unified Approach. Wiley-Interscience, New York, NY.

Louca, L.S., J.L. Stein, G.M. Hulbert, and J.K. Sprague, 1997. Proper Model Generation: An Energy-Based Methodology. Proceedings of the 1997 International Conference on Bond Graph Modeling, pp. 44-49, January, Phoenix, AZ. Published by SCS, ISBN 1-56555-103-6, San Diego, CA.

Louca, L.S. and J.L. Stein, 1998. "Physical Interpretation of Reduced Bond Graphs". Proceedings of the 2nd IMACS International Multiconference: Computational Engineering in Systems Applications (CESA'98). Hammamet, Tunisia.

Louca, L.S., J.L. Stein and G.M. Hulbert, 1998. A Physical-Based Model Reduction Metric with an Application to Vehicle Dynamics. The 4th IFAC Nonlinear Control Systems Design Symposium (NOLCOS 98). Enschede, The Netherlands.

Louca, L.S., 1998. An Energy-Based Model Reduction Methodology for Automated Modeling. Ph.D. Thesis. The University of Michigan. Ann Arbor, MI.

Pacejka, H.B. and C.G.M. Tol, 1983. A Bond Graph Computer Model to Simulate the 3-D Dynamic Behavior of a Heavy Truck. Modeling and simulation in engineering, IMACS World Congress on Systems Simulation and Scientific Computation. Montreal, Quebec.

Pacejka, H.B. and E. Bakker, 1993. Tyre Models for Vehicle Dynamics Analysis. Proceedings of the 1st International Colloquium on Tyre Models for Vehicle Dynamics Analysis Delft, Netherlands

Phillips, A.W., and D.N. Assanis, 1989. A PC-Based Vehicle Powertrain Simulation for Fuel Economy and Performance Studies - VPS, International Journal of Vehicle Design, 10:6, 639-658.

Rosenberg, R.C., and D.C. Karnopp, 1983. Introduction to Physical System Dynamics. McGraw-Hill, New York, NY.

9. APPENDIX

Rank	Cumulative [%]	Activity [%]	Element Name
1	42.3547	4.2355E-01	Vehicle\body\Mx
2	54.0910	1.1736E-01	Vehicle\tire_rear\B_brake
3	65.1828	1.1092E-01	Vehicle\tire_front\B_brake
4	75.6723	1.0490E-01	DT\TC\FluidCoupling
5	81.8427	6.1704E-02	Vehicle\body\Raero
6	84.6156	2.7729E-02	Vehicle\axle_rear\Mx
7	87.2761	2.6605E-02	Vehicle\tire_rear\B_slip
8	89.1540	1.8780E-02	Vehicle\tire_rear\B_rolling
9	90.8436	1.6895E-02	Vehicle\tire_front\B_slip
10	92.4196	1.5760E-02	Vehicle\axle_front\Mx
11	93.9316	1.5121E-02	DT\Prop_Diff\differential
12	94.9927	1.0611E-02	Vehicle\tire_front\B_rolling
13	95.8307	8.3792E-03	DT\Prop_Diff\B_churning
14	96.6569	8.2627E-03	Vehicle\tire_rear\Jwheel
15	97.2786	6.2170E-03	Engine\J
16	97.8894	6.1074E-03	DT\Transmission\gear
17	98.3414	4.5200E-03	Vehicle\tire_front\Jwheel
18	98.7923	4.5096E-03	DT\Transmission\T_charging
19	99.1388	3.4643E-03	DT\Transmission\I1
20	99.4778	3.3903E-03	DT\Transmission\B_churning
21	99.6641	1.8635E-03	DT\Transmission\I2
22	99.7519	8.7739E-04	DT\TC\I_turbine
23	99.8369	8.5015E-04	Vehicle\axle_front\C_susp
24	99.8645	2.7626E-04	Vehicle\tire_front\C_tire
25	99.8917	2.7169E-04	Vehicle\axle_rear\C_susp
26	99.9158	2.4123E-04	DT\Prop_Diff\I_axle
27	99.9313	1.5503E-04	DT\Prop_Diff\I2
28	99.9457	1.4344E-04	Vehicle\tire_rear\C_tire
29	99.9589	1.3280E-04	Vehicle\frame\My
30	99.9683	9.4054E-05	DT\Prop_Diff\C_axle_out
31	99.9763	7.9473E-05	DT\Prop_Diff\I1
32	99.9838	7.5482E-05	DT\Prop_Diff\I3
33	99.9896	5.7976E-05	Vehicle\frame\J
34	99.9927	3.0673E-05	DT\Transmission\C2
35	99.9941	1.4240E-05	DT\Prop_Diff\C1
36	99.9955	1.3591E-05	DT\Prop_Diff\C2
37	99.9967	1.2248E-05	DT\Prop_Diff\C_axle_in
38	99.9976	8.5697E-06	Vehicle\axle_rear\My
39	99.9982	6.2376E-06	DT\Prop_Diff\B_axle_out
40	99.9988	6.0076E-06	Vehicle\axle_front\B_susp
41	99.9993	5.5139E-06	DT\Transmission\C3
42	99.9999	5.1464E-06	Vehicle\axle_front\My
43	99.9999	4.9906E-07	Vehicle\axle_rear\B_susp
44	99.9999	4.0820E-07	DT\Transmission\B2
45	100.0000	1.9998E-07	DT\Transmission\C1
46	100.0000	1.6112E-07	Vehicle\tire_front\B_tire
47	100.0000	6.4768E-08	DT\Prop_Diff\B_axle_in
48	100.0000	5.1618E-08	DT\Prop_Diff\B1
49	100.0000	3.2226E-08	DT\Prop_Diff\B2
50	100.0000	3.1844E-08	Vehicle\tire_rear\B_tire
51	100.0000	5.2118E-09	DT\Transmission\B3
52	100.0000	1.3387E-09	DT\Transmission\B1
53	100.0000	1.2363E-09	Vehicle\tire_rear\B_bearing
54	100.0000	1.0532E-09	Vehicle\tire_front\B_bearing
55	100.0000	1.5733E-10	Engine\B